FULL PAPER

Injectable Hydrogels from Triblock Copolymers of Vitamin E-Functionalized Polycarbonate and Poly(ethylene glycol) for Subcutaneous Delivery of Antibodies for Cancer Therapy

Ashlynn L. Z. Lee, Victor W. L. Ng, Shujun Gao, James L. Hedrick, and Yi Yan Yang**

In this study, 'ABA'-type triblock copolymers of vitamin E-functionalized polycarbonate and poly(ethylene glycol), i.e., $VitE_m$-PEG-$VitE_m$, with extremely short hydrophobic block $VitE_m$, are synthesized and employed to form physically cross-linked injectable hydrogels for local and sustained delivery of Herceptin. The hydrogels are formed at low concentrations (4–8 wt%). By varying polymer composition and concentration, the rheological behavior, porosity, and drug release properties of hydrogels are readily tunable. The in vitro antitumor specificity and efficacy of Herceptin in hydrogel and solution are investigated by MTT assay against normal and human breast cancer cell lines with different HER2 expression levels. The results demonstrate that the Herceptin-loaded hydrogel is specific towards HER2-overexpressing cancer cells and cytotoxic action is comparable to that of the Herceptin solution. The biocompatibility and biodegradability of hydrogel are evaluated in mice with subcutaneous injection by histological examination. It is observed that the hydrogel does not evoke a chronic inflammatory response and degrades within 6 weeks post administration. Biodistribution and anti-tumor efficacy studies performed in BT474 tumor-bearing mice show that single subcutaneous injection of Herceptin-loaded hydrogel at a site close to the tumor enhances the retention of the antibody within the tumor. This leads to superior anti-tumor efficacy as compared to intravenous (i.v.) and subcutaneous (s.c.) delivery of Herceptin in solution. The tumor size shrank by 77% at Day 28. When the hydrogel is injected at a distal location away from the tumor site, anti-tumor efficacy is similar to that of weekly i.v. injections of Herceptin solution over 4 weeks, with the number of injections reduced from 4 to 1. These findings suggest that this hydrogel has great potential for use in subcutaneous and sustained delivery of antibodies to increase therapeutic efficacy and/or improve patient compliance.

1. Introduction

According to a 2008 World Health Organization (WHO) survey, breast cancer comprises of 22.9% of all cancers (excluding non-melanoma skin cancer) and its mortality rate is around 13.7% worldwide.[1] In Europe, the incident rate of breast cancer is even higher, reaching 28%. Treatment of breast cancer may vary according to the size, stage and rate of growth, as well as the type of tumor. There are currently three main categories of adjuvant, or post-surgery, therapies available; they include hormone-blocking therapy, chemotherapy and monoclonal antibodies (mAbs) therapy. The latter involves the utilization of mAbs to target specific cells or proteins towards the treatment of disease by inducing, enhancing or suppressing an immune response. It can be used in conjunction with either hormone-blocking therapy or chemotherapy to enhance the efficacy of cancer treatment.

Studies have shown that the human epidermal growth factor receptor 2 (HER2) genes are amplified and/or overexpressed in 20–25% of invasive breast cancer and has been found to be a worse prognosis than those having HER2-negative tumors, as demonstrated by significantly lower survival rates.[2,3] In these cases, unrestrained growth and division of cells in the breasts are most likely to occur, thus increasing the incidence of cancer development. Herceptin is a recombinant humanized mAb that can selectively bind to HER2 proteins and reduce signaling from multiple pathways, including the PI3 kinase (PI3K) and MAP kinase (MAPK) cascades. This leads to cell cycle arrest and apoptosis, regulating uncontrollable cancer growth.[4] Herceptin is also a US Food and Drug Administration (FDA)-approved therapeutic for the treatment of HER2+ breast cancer. Intravenous administration is the current mode of Herceptin delivery in most clinics. However, many controversies surround the optimal mode of delivery in terms of duration and dosage.[5] Recently, F Hoffmann-La Roche has reported a phase 3 clinical trial (HannaH study) involving the subcutaneous (s.c.)

Dr. A. L. Z. Lee, Dr. V. W. L. Ng, Dr. S. Gao, Dr. Y. Y. Yang
Institute of Bioengineering and Nanotechnology
31 Biopolis Way, The Nanos
Singapore 138669, Singapore
Tel: 65-6824-7106, Fax: 65-6478-9084
E-mail: yyyang@ibn.a-star.edu.sg
Dr. J. L. Hedrick
IBM Almaden Research Center
650 Harry Road, San Jose, CA 95120, USA
Tel: 1-408-927-1632, Fax: 1-408-927-3310
E-mail: hedrick@us.ibm.com

DOI: 10.1002/adfm.201301307

(versus intravenous (i.v.)) administration of (neo)adjuvant Herceptin in patients with HER2+ breast cancer.[6] The formulation consists of a fixed dose of Herceptin and recombinant human hyaluronidase (rHuPH-20), a class of enzymes that temporarily degrades interstitial hyaluronan in the subcutaneous space, as an excipient. In this study, it was found that therapeutic efficacy of subcutaneous delivery of Herceptin was comparable to the traditional intravenous route. In addition, the authors also pointed out the potential of such therapy, such as, improved patient convenience, better compliance, reduced pharmacy preparation times, and optimization of medical resources.[7]

Hydrogels produced from the self-assembly of synthetic polymers have an inexhaustible potential to serve as drug delivery matrix for localized administration. Recent developments in polymer chemistry have enabled polymers to be synthesized with well-controlled composition and architecture. Highly versatile orthogonal functionalization strategies also allow gelation of such polymers and containment of drug payload through one or a combination of the following association mechanisms such as hydrophobic interactions, ionic interactions, hydrogen bonding, physical entanglement of macromolecules and chemical cross-linking of the matrix.[8–10] A number of physical gel systems have been formulated using the 'ABA'-type triblock copolymers and the polymeric amphiphiles can be designed with either the 'A' or 'B' constituent blocks to be hydrophilic or hydrophobic. Many of such systems engages the use of poly(ethylene glycol) (PEG) as the uncharged hydrophilic constituent block due to its biocompatibility, FDA approval and commercial availability with a variety of telechelic end-groups. Some commonly used hydrophobic components include biodegradable poly(L-lactic acid) (P_LLA), poly(L-glycolic acid), poly(lactic-*co*-glycolic acid) (PLGA) and poly(caprolactone). They can either form the middle 'B' block (e.g. PEG-PLGA-PEG[11]) or as the terminus 'A' blocks (e.g. P_LLA-PEG-P_LLA[12,13]). Aqueous mixture of enantiomeric triblock copolymers (e.g. P_LLA-PEG-P_LLA and P_DLA-PEG-P_DLA) could also form physical gels via stereocomplexation.[14] Most 'ABA'-type polymers require high concentration and/or hydrophobic content for hydrogel formation. For instance, P_LLA-PEG-P_LLA containing high lactide content of 17 to 37 wt.% require a minimum concentration of 16 wt.% for gelation.[12] Such high hydrophobic compositions could give rise to adverse physiological effects during in vivo degradation. Thus, it is desirable to develop biodegradable polymeric materials that can form hydrogels at a low concentration.

In this study, we have selected vitamin E-functionalized polycarbonates as the hydrophobic block to synthesize 'ABA'-type copolymers because polycarbonates are biodegradable and their degradation products are non-toxic.[15,16] In addition, vitamin E (α-tocopherol) has been reported to have antioxidant function,[17] and the introduction of hydrophobic α-tocopherol moiety into the polymer would have a significant influence on the gelation and rheological properties of the hydrogels. Vitamin E-functionalized polycarbonates were synthesized by organocatalytic ring-opening polymerization of vitamin E-functionalized carbonate using PEG as a macroinitiator. Notably, the hydrophobic content can easily be tuned by controlling the feed ratio of the vitamin E-containing monomer. These triblock polymers are capable of forming hydro- and organo-gels depending on the hydrophobic/hydrophilic balance of the polymers and solvent composition. Importantly, both vitamin E and PEG are biocompatible and FDA-approved chemical compounds and this gives the hydrogel system added advantage in the realization of pharmaceutical application. These physically cross-linked vitamin E-functionalized hydrogels were characterized for rheological behavior, morphology and Herceptin release properties. The in vitro antitumor specificity and efficacy was investigated by MTT assays against normal and human breast cancer cell lines with different HER2 expression levels. In vivo biocompatibility and biodegradability of the subcutaneously injected hydrogel was also investigated *via* histological examination. Furthermore, animal studies performed using a single subcutaneous injection of Herceptin-loaded hydrogel at a site close to the tumor displayed superior anti-tumor efficacy as compared to i.v. and s.c. injections of Herceptin solution, thereby demonstrating great potential as a post-operative therapy. The Herceptin-loaded hydrogel may also be incorporated into the standard therapeutic regimen to improve patient compliance as the anti-tumor efficacy of hydrogel administered once at a distal location away from the tumor was comparable to that of weekly i.v. injection of Herceptin solution over 4 weeks.

2. Results and Discussion

2.1. 5-Methyl-5-(α-tocopheryl)carboxyl-1,3-dioxan-2-one (MTC-VitE) Monomer and Polymer Synthesis

The synthesis of MTC-VitE monomer is simple and straightforward, which involves the direct coupling of MTC-Cl with α-tocopherol in the presence of triethylamine (**Figure 1**A). The yield of the desired product is 53%; prolonged stirring did not result in significant decomposition. The use of α-tocopherol allows for the creation of a hydrophobic cyclic carbonate.

The organocatalytic ring opening polymerization (ROP) of MTC-VitE, initiated by HO-PEG-OH, was achieved using 1,8-diazabicyclo[5,4,0]undec-7-ene (DBU)/N-(3,5-trifluoromethyl)phenyl-N′-cyclohexylthiourea (TU) catalysts combination (Figure 1A). All ROPs were incomplete and the conversion efficiency was around 60% as analyzed by their respective ^{1}H NMR. The excess monomers and reagents were simply removed by repeated precipitation with diethyl ether. Finally, 'ABA'-type polymers with various compositions were obtained (**Table 1**). The polymers are coded based on the molecular weight of PEG used and the actual degree of polymerization (DP_m) of MTC-VitE obtained according to ^{1}H NMR analysis, for example, $VitE_{1.25}$-PEG(20k)-$VitE_{1.25}$. All polymers are subjected to gel permeation chromatography (GPC) analysis and all of them are unimodal having narrow molecular weight distribution with polydispersity index (PDI) < 1.2, indicating well-controlled polymerization. The hydrophobicity of the polymer can be fine-tuned easily by varying the feed ratio of the MTC-VitE moiety; for instance, $VitE_{1.25}$-PEG(20k)-$VitE_{1.25}$ and $VitE_{2.5}$-PEG(20k)-$VitE_{2.5}$ form hydrogels easily while $VitE_{6.5}$-PEG(20k)-$VitE_{6.5}$ and $VitE_{8.5}$-PEG(20k)-$VitE_{8.5}$ can only yield organogels. $VitE_{1.25}$-PEG(10k)-$VitE_{1.25}$ and $VitE_{2.5}$-PEG(10k)-$VitE_{2.5}$ did not give rise to the desired gelation effect under similar conditions. Figure 1B illustrates the hydrogel formation resulting from

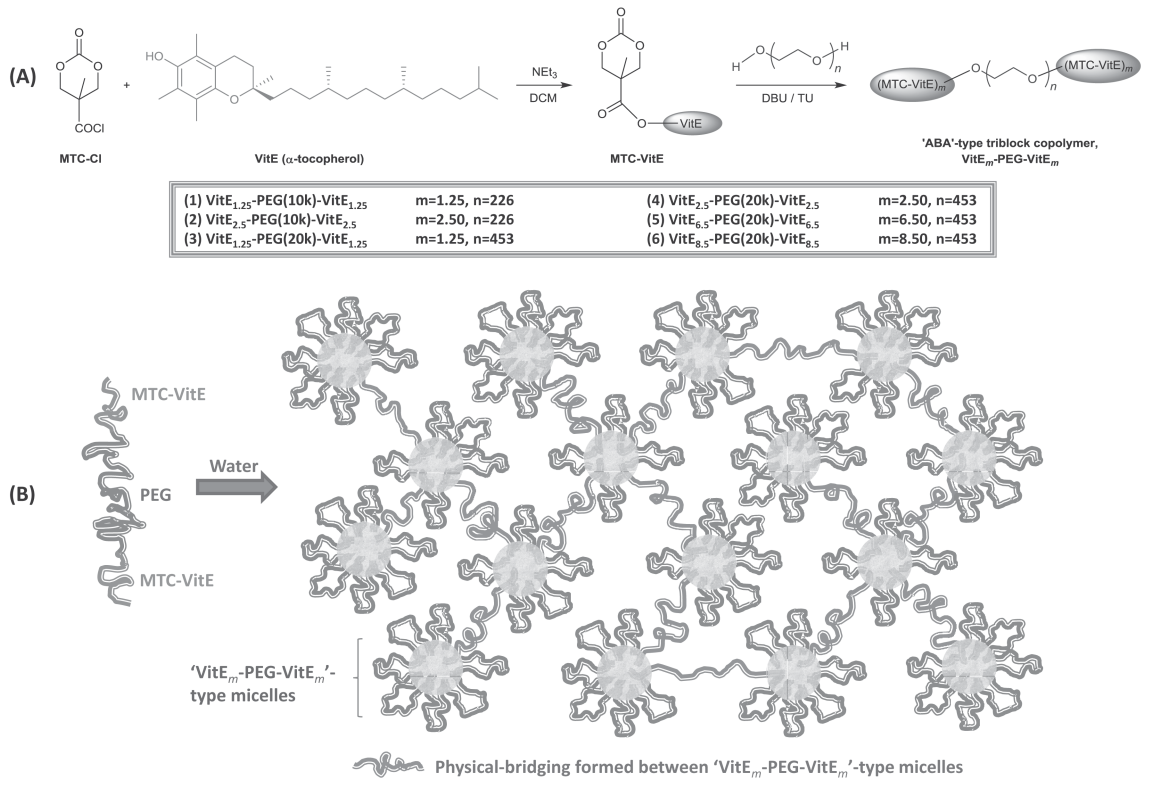

Figure 1. A) Synthesis of MTC-VitE monomer and its ROP initiated by HO-PEG-OH. B) Hydrogel formation from physical cross-linking of $VitE_m$-PEG-$VitE_m$ micelles.

physical cross-linking between 'flower-like' micellar networks arising from the 'ABA' triblock copolymer.

2.2. Rheological Properties of Hydrogels

The effects of concentration, hydrophobic/hydrophilic balance and chemical composition of the amphiphilic copolymers on rheological properties of hydrogels were investigated using dynamic mechanical analysis. Polymer concentration strongly affected the storage modulus G′ of the hydrogel (**Figure 2**A and B) where one fold increment of concentration (4 to 8 wt%) resulted in 4 to 10 times higher G′ values. In particular, 8 wt% of $VitE_{2.5}$-PEG(20k)-$VitE_{2.5}$ gel had storage modulus G′ of ~12 000 Pa, which is nearly 10-fold of the 4 wt% gel (G′ = 1400 Pa). The influence in balancing the hydrophobic and hydrophilic components of the polymers on the gel stiffness can be seen at higher polymer concentration. By increasing the VitE units from 1.25 to 2.5 at a polymer concentration of 8 wt% gave rise to a 1-fold increase in the storage modulus G′ (~5000 vs. ~12 000 Pa). The molecular weight between effective cross-links M_c was determined (Table S1). Hydrogels with increasing polymer concentration displayed lower M_c values, which corresponds to lower molecular weight between cross-links and higher cross-link density.[18] In addition, we also synthesized two control polymers without VitE, TMC_5-PEG(20k)-TMC_5 (TMC = 1,3-trimethylene carbonate) and $(MTC\text{-}OBn)_2$-PEG(20k)-$(MTC\text{-}OBn)_2$ (MTC-OBn = 5-methyl-5-benzylcarboxyl-1,3-dioxan-2-one) (see Section S1.1

Table 1. Composition of $VitE_m$-PEG-$VitE_m$ triblock copolymers.

Code	M_w^{PEG} [kDa][a)]	MTC-VitE to PEG Feed Ratio	DP_m[b)]	f^{PEG}[c)]
$VitE_{1.25}$-PEG(10k)-$VitE_{1.25}$	10	4	1.25	87.2
$VitE_{2.5}$-PEG(10k)-$VitE_{2.5}$	10	8	2.5	77.3
$VitE_{1.25}$-PEG(20k)-$VitE_{1.25}$	20	4	1.25	93.1
$VitE_{2.5}$-PEG(20k)-$VitE_{2.5}$	20	8	2.5	87.2
$VitE_{6.5}$-PEG(20k)-$VitE_{6.5}$	20	20	6.5	72.3
$VitE_{8.5}$-PEG(20k)-$VitE_{8.5}$	20	30	8.5	66.6

[a)]Molecular weight data from supplier; [b)]Average degree of polymerization of MTC-VitE, DP_m, based on ^{1}H NMR spectroscopy; [c)]Weight fraction of PEG, $f^{PEG} = M_w^{PEG} / (M_w^{PEG} + 2 \times DP_n \times 588.83)$.

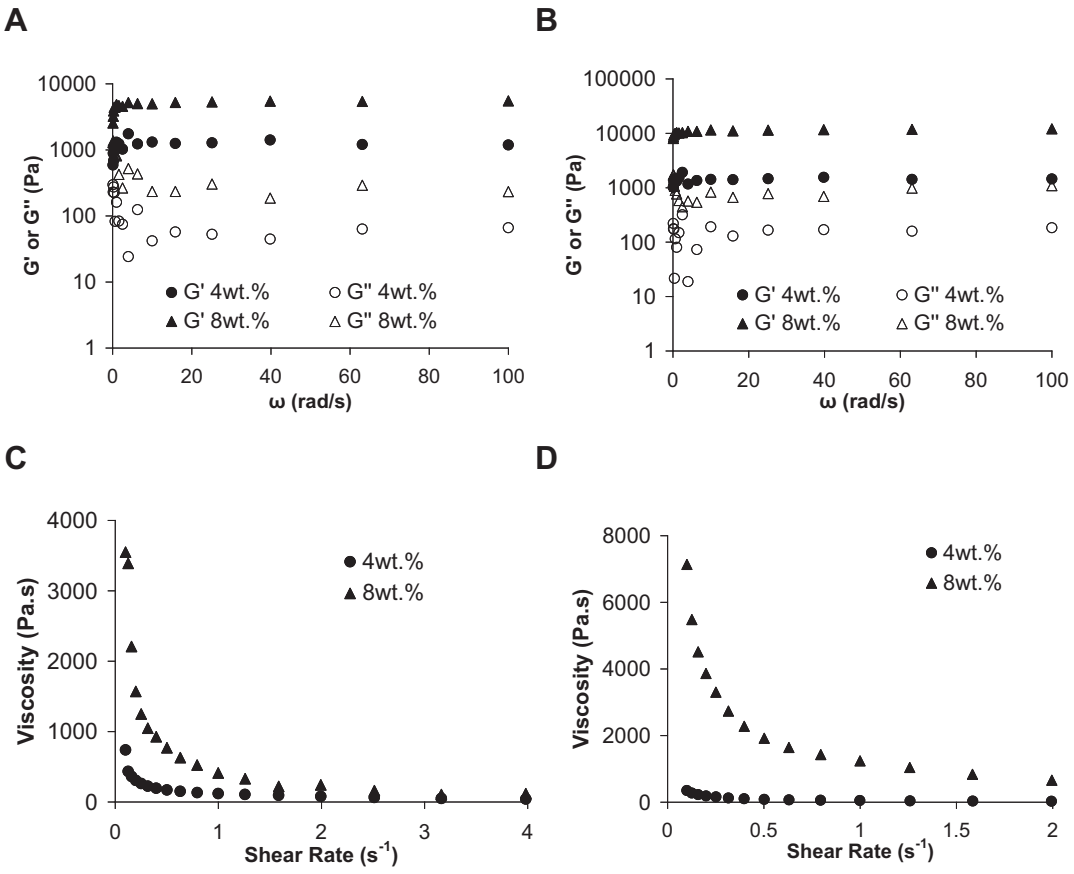

Figure 2. Frequency and flow sweep of storage (G′) and loss (G″) moduli of $VitE_{1.25}$-PEG(20k)-$VitE_{1.25}$ (A and C) and $VitE_{2.5}$-PEG(20k)-$VitE_{2.5}$ (B and D) hydrogels with different polymer concentrations at 25 °C.

in the Supporting Information-SI), with similar weight fraction of PEG composition for comparison with $VitE_{1.25}$-PEG(20k)-$VitE_{1.25}$. These polymers did not gel for even up to 30 wt.%, indicating that the presence of vitamin E in the hydrophobic blocks of the triblock copolymers is indeed essential for gelation to occur at low concentrations (4–8 wt%). Tew and co-workers also reported a series of P_LLA-PEG-P_LLA polymers that required high gelation concentrations (~17 – 37%).[12]

The reduction in viscosity of hydrogels with increasing shear rate at 25 °C is shown in Figure 2C and D. This demonstrated the shear-thinning properties of the hydrogels, which resulted from the disruption of physical cross-links between the polymer chains with the application of shear stress. In order for hydrogels to be used as injectable drug depot, it is essential that the disrupted solution phase could rapidly reverse back into a gel after shear force terminates. To study this property, a dynamic step strain amplitude test (γ = 0.2 or 100%) was applied on the $VitE_{1.25}$-PEG(20k)-$VitE_{1.25}$ (4 wt%) hydrogel. **Figure 3** shows that the initial G′ was ~1400 Pa at a small strain (γ = 0.2%). When subjected to a high strain (γ = 100%), the G′ value immediately decreased by more than 20 times to ~67 Pa. After 200 s of the continuous stress, the strain was returned to γ = 0.2% and the G′ was immediately recovered to ~1400 Pa without any loss. This reversibility of rheological behavior of the hydrogel is extremely advantageous for use as an injectable matrix for delivery of therapeutics.

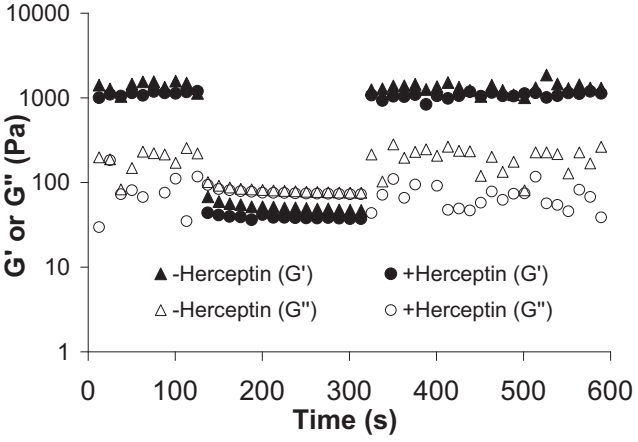

Figure 3. Dynamic step strain amplitude test (γ = 0.2 or 100%) for blank and Herceptin-loaded $VitE_{1.25}$-PEG(20k)-$VitE_{1.25}$ (4 wt%) hydrogel. 10 g/L Herceptin was loaded into the hydrogel.

2.3. SEM Studies of Hydrogels

SEM images of hydrogels (**Figure 4**) show that the cross-section morphology and porosity of the hydrogel network was strongly influenced by polymer concentration and hydrophobic/

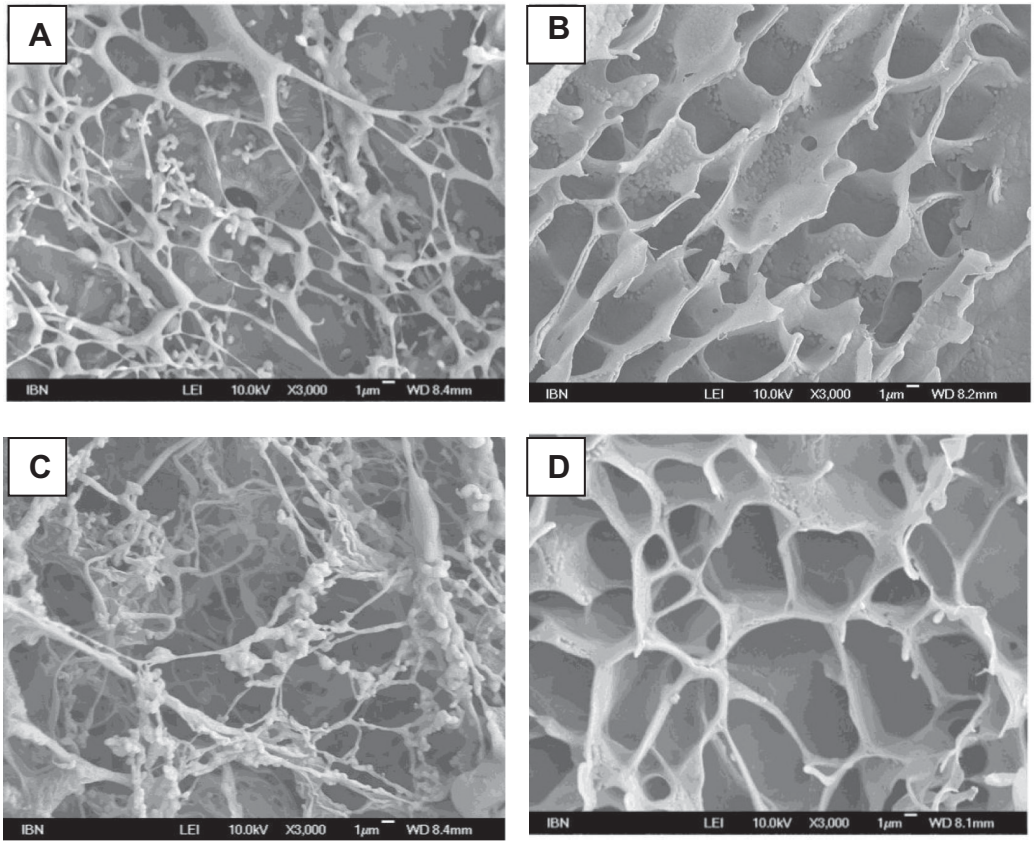

Figure 4. SEM images of cryo-fixed 4 and 8 wt% of $VitE_{1.25}$-PEG(20k)-$VitE_{1.25}$ (A and B) and $VitE_{2.5}$-PEG(20k)-$VitE_{2.5}$ (C and D) hydrogels. The hydrogels were formed in DI water and rapidly transferred into a chamber filled with liquid nitrogen. This was then followed by a day of freeze-drying process. Scale bar represents 1 μm.

hydrophilic balance. Spherical structures with diameters below 1 μm could be aggregates of micelles self-assembled from the polymers. As the concentration increased above a certain threshold value, nanophase separation within the gel matrix took place and the hydrogels occurred as nanophase-separated sponge structures.[19] The porosity of the sponge structures appeared to vary with polymer concentration. The 8 wt% hydrogels (Figure 4B,D) were less porous compared to the hydrogels formed at 4 wt% (Figure 4A,C). This observation correlates to the M_c values where the hydrogels formed at higher polymer concentration displayed lower M_c values and higher cross-link density (Table S1).

2.4. Herceptin Release

The release of Herceptin from the hydrogels formed at 4 wt% was studied in PBS at 37 °C. From **Figure 5**A, Herceptin release was faster from $VitE_{2.5}$-PEG(20k)-$VitE_{2.5}$ hydrogel than that from $VitE_{1.25}$-PEG(20k)-$VitE_{1.25}$ hydrogel, and 90% of Herceptin is released in 2 days from $VitE_{2.5}$-PEG(20k)-$VitE_{2.5}$ hydrogel while the same amount of release is completed only in 12 days for the $VitE_{1.25}$-PEG(20k)-$VitE_{1.25}$ hydrogel and this finding is consistent with other reported protein release studies where the proportion of hydrophilic PEG to hydrophobic component strongly influences drug release kinetics.[20,21] The sustained release of Herceptin provided by $VitE_{1.25}$-PEG(20k)-$VitE_{1.25}$ hydrogel and ease in injection through a 23G needle make it an appropriate candidate for local delivery of Herceptin. Therefore, further studies were carried out using this hydrogel formulation.

2.5. Cytotoxicity of Herceptin Delivered by Hydrogels Against Various Cell Lines

Herceptin loaded in $VitE_{1.25}$-PEG(20k)-$VitE_{1.25}$ hydrogel (4 wt%) was tested against HER2/neu-overexpressing human breast cancer BT474 cells, low HER2/neu- expressing human breast cancer MCF7 cells[22] and human dermal fibroblasts (HDF) to investigate the treatment specificity as well as in vitro biocompatibility of the hydrogel. As shown in Figure 5B, 48 h treatment was insufficient for Herceptin to exert sufficient killing effect on BT474 cells as the cells still remained viable at ~65% even at the highest Herceptin concentration tested (i.e., 5 g/L). Interestingly, when the treatment was extended to 120 h, the IC_{50} of Herceptin delivered using the hydrogel was drastically reduced to 0.02 g/L, whereas the blank hydrogel has minimal cytotoxicity. The IC_{50} of Herceptin was lower with the solution formulation at <0.005g/L. The higher IC_{50} value of the hydrogel

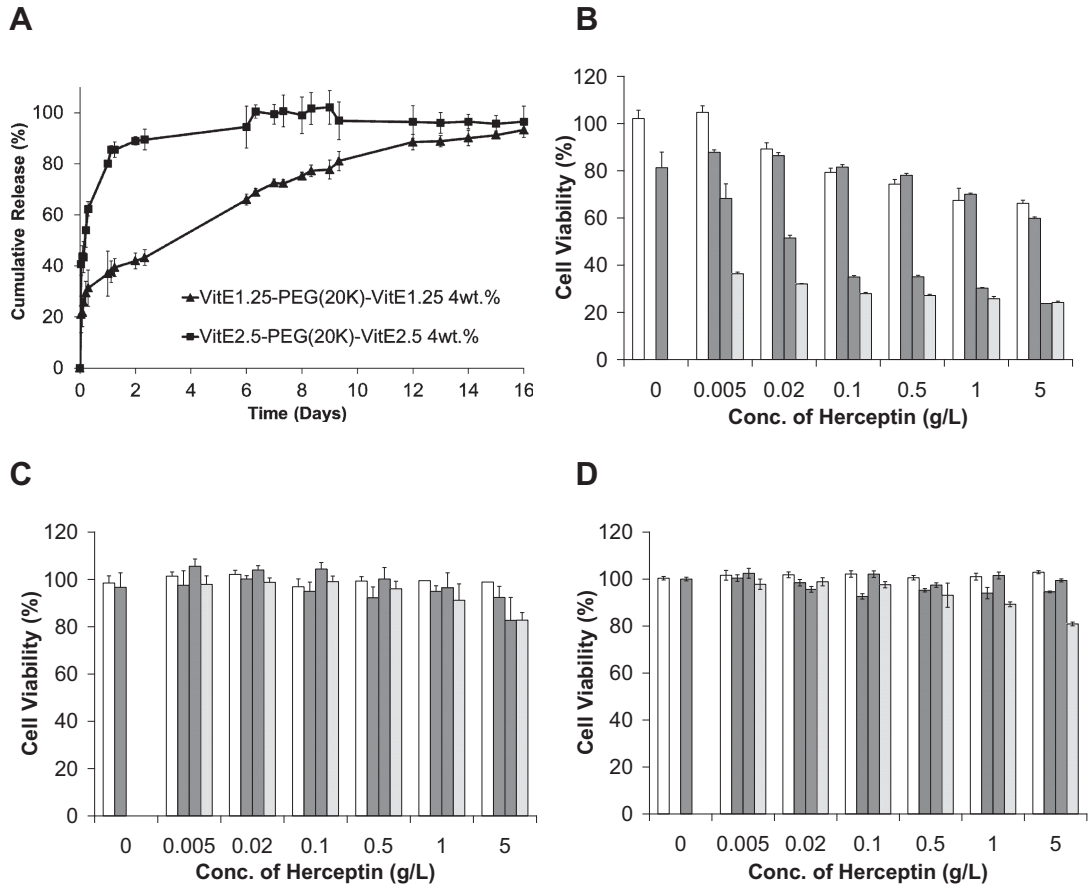

Figure 5. A) Release profiles of Herceptin from $VitE_{1.25}$-PEG(20k)-$VitE_{1.25}$ and $VitE_{2.5}$-PEG(20k)-$VitE_{2.5}$ (4 wt%) hydrogels as a function of time. Viability of B) BT474, C) MCF7, and D) HDF cells after treatment with various Herceptin formulations.

formulation could be due to the release kinetics of Herceptin from the hydrogel. About 50% of the initial amount of Herceptin from the hydrogel was released by 5 days (i.e., 120 h), and therefore, the cumulative cytotoxic effect of Herceptin-loaded hydrogel on BT474 cells was lower over the 5-day period as compared to the bolus (one-time) delivery of Herceptin solution. Nonetheless, the Herceptin-loaded hydrogel was highly effective in killing BT474 cells at high Herceptin concentrations (≥1 g/L), where more than 70% of the cells were killed in 120 h. At the higher Herceptin concentration (5 g/L), the amount of Herceptin released from the hydrogels could have exceeded the effective therapeutic dose, resulting in comparable cytotoxicity between the hydrogel and solution formulations of Herceptin. Pharmacokinetic studies have shown that Herceptin has a half-life of 6.2 to 8.3 days,[23,24] and with the sustained release profile of Herceptin from the hydrogel for more than 2 weeks, it is anticipated that the hydrogel would be able to deliver a continuous supply of antibody in vivo and eradicate HER2+ tumors.

In MCF7 cells, Herceptin delivered either in the hydrogel or solution formulation shows negligible cytotoxic effect with more than 80% cell viability even after 120 h treatment at up to Herceptin concentration of 5 g/L (Figure 5C). This demonstrates that the Herceptin treatment was specific towards HER2/neu-overexpressing cancer cells. The antibody solution showed slight cytotoxicity against HDF at 5 g/L after 120 h of treatment (Figure 5D). This is not unexpected as epidermal growth factor receptors (EGFR/ErbB) are present on the HDF cells and even though they are not overexpressed like in BT474 cells, it is possible that the interactions of Herceptin with the receptors can cause slight hinderence HDF proliferation.[25–28] Furthermore, the blank hydrogel showed no cytotoxicity on HDF even after 120 h of treatment (Figure 5D).

2.6. In vivo Biocompatibility and Gel Degradation Studies

In order for the vitamin E-functionalized polymeric hydrogel to serve as drug delivery depot, it is crucial that the material is biocompatible in vivo. To evaluate this property, subcutaneous injection of the blank $VitE_{1.25}$-PEG(20k)-$VitE_{1.25}$ hydrogel 4 wt% was carried out in mice and optical photomicrographs of histological sections of the hydrogel and its surrounding tissue were examined at 1, 2, 4, and 6 weeks post injection (**Figure 6** and S1A). These were compared against histological samples that were excised from untreated mice (Figure S1B). The inflammatory cells were identified by immunohistochemical staining using an anti-CD45 antibody that recognizes the leukocyte common antigen (CD45).[29,30] The slides were counterstained with hematoxylin to visualize cell nuclei. Within 2 weeks post injection, the hydrogel remained mostly intact (bracketed regions and arrows in Figure 6) and some inflammatory cells (indicated by brown DAB stains) had infiltrated into the hydrogel. On the contrary, CD45+ cells were not observed in the similar subcutaneous region of untreated mice (Figure S1B). At 4 weeks, the thickness of the hydrogel had reduced, indicating degradation of the hydrogel. By 6 weeks, the hydrogel had mostly dissociated and was not clearly visible under gross examination (Figure S1A). In addition, CD45+ cells were hardly found, showing that the inflammatory response was only temporary and did not progress to a chronic stage.

2.7. Biodistribution of Herceptin Delivered Using Different Formulations

The biodistribution of Herceptin following administration in hydrogel and solution formulations was examined in a BT474-tumor bearing mouse model by non-invasive fluorescent imaging at various time points up to 13 days after injection. The mice were sacrificed at the end of the experiment to provide a semi-quantitative estimation of the distribution of Herceptin in individual tissues using the heat map (**Figure 7**). Comparison between subcutaneous (s.c.) and intravenous (i.v.) injections of Heceptin solution showed that the subcutaneous injection was more favorable. Intravenous injection method resulted in Herceptin accumulation mainly within organs such as kidneys, liver and lungs,[31,32] but only a very little amount seen in the tumor tissue. When Herceptin solution was injected subcutaneously close to the tumor site, the antibody accumulated to a greater extent in the tumor compared to that in the i.v. injection case. This is most likely due to the proximity to the tumor tissue, which might allow accessibility for Herceptin to diffuse to the tumor. For both s.c. and i.v. administrations of Herceptin solution, the accumulation of Herceptin in the normal tissues showed a similar trend, with the highest amount residing in the kidneys (Figure 7). On the other hand, the hydrogel formulation provided localized delivery of Herceptin, leading to a high amount of Herceptin accumulation within the tumor and very little amount in the other organs. The biodistribution patterns of various formulations will likely influence their anti-tumor efficacy.

2.8. In vivo Antitumor Efficacy and Histological Examination

To understand the therapeutic efficacy of Herceptin delivery via different routes of administration, Herceptin-loaded $VitE_{1.25}$-PEG(20k)-$VitE_{1.25}$ hydrogel (4 wt%) injected s.c. was compared to both i.v. and s.c. administration of Herceptin solution in the BT474-tumor bearing mouse model. The mice were divided into 5 groups consisting of: control injected on the first day of treatment (Day 0) with HPLC grade water (s.c.); Herceptin in solution (i.v.); Herceptin in solution (s.c.); blank and Herceptin-loaded hydrogels (s.c.). Subcutaneous injections were performed once per mouse at ~1 cm away from tumor sites. The administrated dosage of Herceptin was 30 mg/kg in 150 μL for all formulations. Changes in tumor size with time (**Figure 8**A) show that the tumor growth inhibition resulting from the solution and hydrogel formulations were different. The mice that were treated with blank hydrogel had similar average tumor volume compared to the control group ($P = 0.56$). This indicates that the VitE-functionalized hydrogel did not exert any cytotoxic effect on the tumors. In sharp contrast, the Herceptin-loaded hydrogel resulted in significant tumor reduction of 77% ($P = 0.01$) compared to the control group. It is noteworthy that mice treated with the hydrogel were the only group that showed tumor shrinkage by comparing the tumor size on the initial and final day of treatment course ($P < 0.001$). Furthermore, the anti-tumor efficacy was much more pronounced with the hydrogel treatment compared to the treatments with Herceptin solution (both i.v. and s.c.), with P values < 0.005. This is because the hydrogel localized Herceptin at the tumor site at higher levels over a longer period of time (Figure 7) and enabled Herceptin to exert cytotoxic effect against the cancer cells (Figure 5B). All treatment conditions were well tolerated as no weight loss was observed for all mice during the course of treatments (Figure 8B).

Histological examination of tumor excised from the mice at 28 days post injection was carried out. TUNEL assay reveals apoptotic cells (brown DAB stain) by detecting DNA fragmentation resulting from apoptosis. As shown in Figure S2A, tumor cells treated with Herceptin, regardless of the formulation used, were mostly apoptotic (see green arrows, nuclei stained brown), indicating that anti-tumor mechanism was based on Herceptin-induced apoptosis. H&E staining shows that treatment using Herceptin-loaded hydrogel resulted in fewer cells remaining as compared to the control without any treatment and the treatment groups with s.c. and i.v. injection of Herceptin solution (nuclei and cytoplasm were stained blue and pink *via* haematoxylin and eosin respectively). This further illustrates the higher anti-tumor efficacy of s.c. delivery using the hydrogel.

In addition, the anti-tumor efficacy of one-time subcutaneous injection of Herceptin-loaded hydrogel was compared to weekly i.v. and s.c. injections of Herceptin solution. Importantly, the s.c. injections was done at a remote site (~4 cm away from the tumor) to increase clinical relevance of the study. The tumor reduction provided by the hydrogel formulation is significantly greater compared to Herceptin solution (s.c.) (Figure 8C). For the latter group, tumors remained similar size throughout the entire course of treatment ($P = 0.59$) while for the hydrogel treated group, the tumor decreased by 30% ($P = 0.03$) by the end of the treatment. The superior anti-tumor efficacy of the

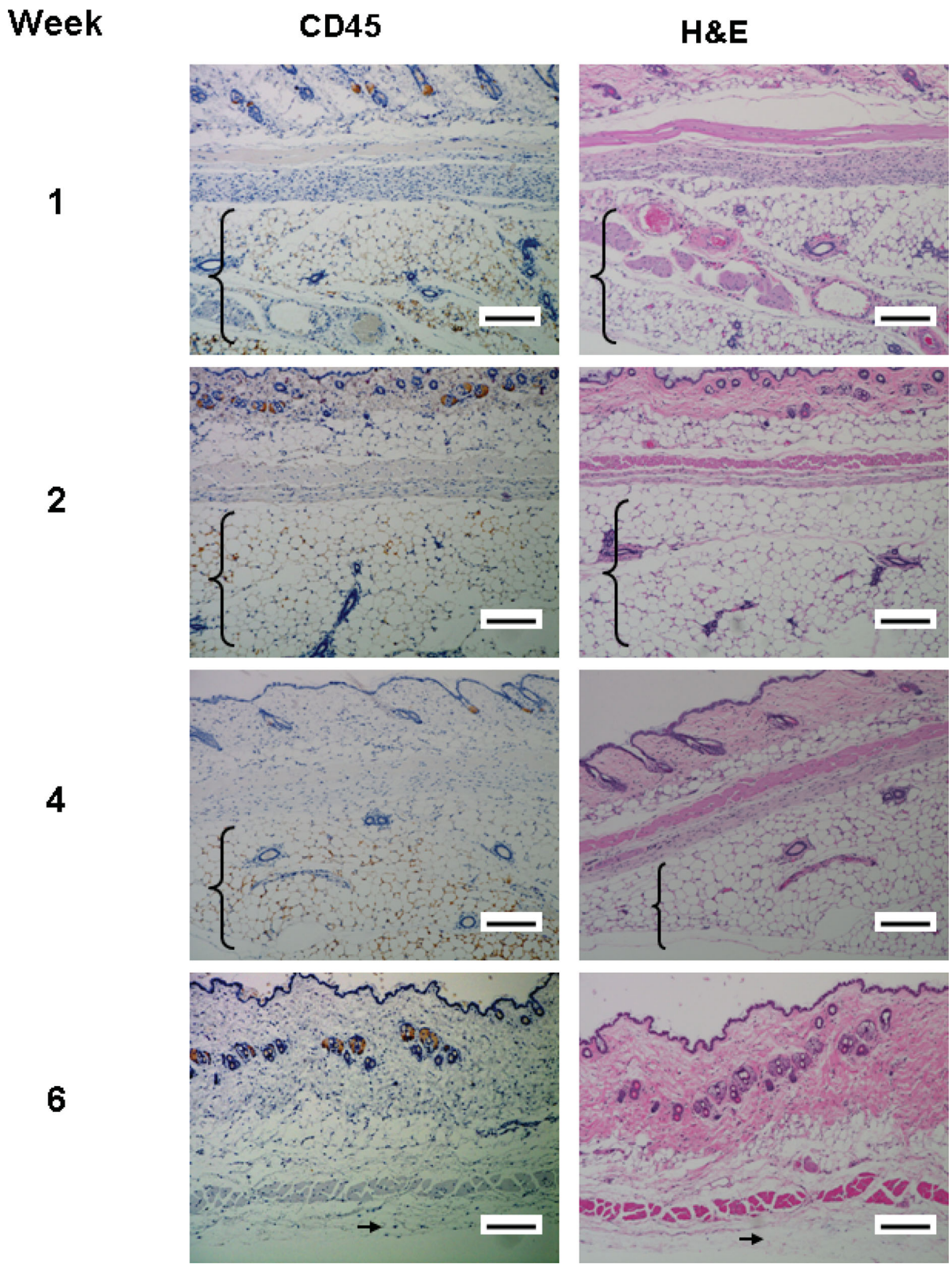

Figure 6. CD45 and H&E staining of blank 4 wt% $VitE_{1.25}$-PEG(20k)-$VitE_{1.25}$ hydrogel and its surrounding tissue retrieved at 1, 2, 4, and 6 weeks post injection. Bracketed regions and arrows indicate the region where hydrogel is present and brown DAB staining indicate the presence of leucocytes. At week 6, the hydrogel has mostly dissociated and could not be distinctly identified. Scale bar represents 200 μm.

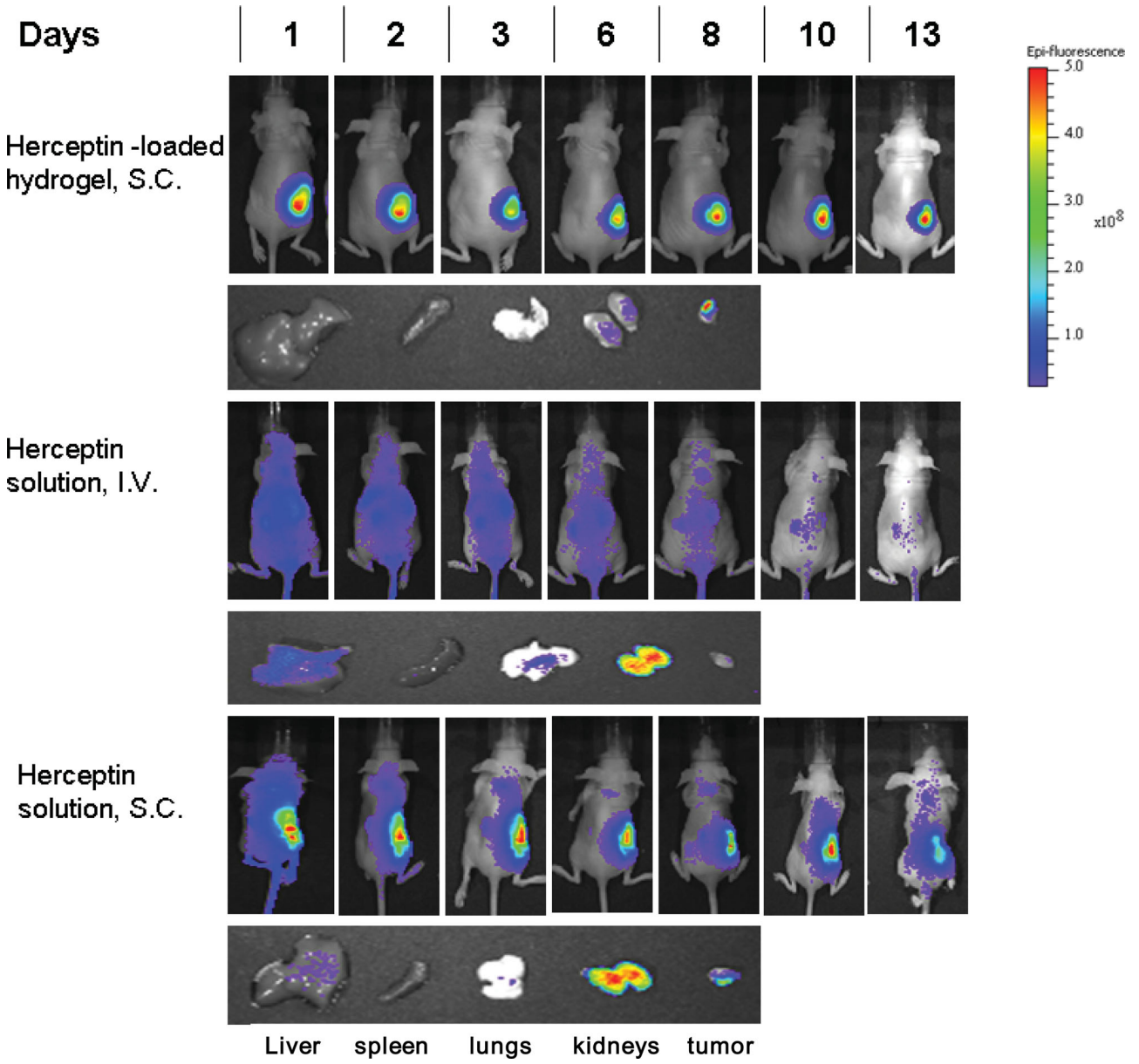

Figure 7. Biodistribution of AlexaFlor790-labeled Herceptin delivered using different formulations. On Day 13, the mice were sacrificed and organs involved in drug clearance and metabolism as well as tumor tissue were excised and imaged. From left: Liver, spleen, lungs, kidneys, tumor.

hydrogel formulation is probably due to the entrapment of Herceptin by the hydrogel network, which enabled the sustained release of the antibody.

During the early phase of treatment, the anti-tumor efficacy of Herceptin-loaded hydrogel was much more pronounced than Herceptin solution (i.v.) as the hydrogel-treated group had 61% tumor shrinkage ($P < 0.001$) by Day 3 while the latter group only began to show reduction in tumor size at > 2 weeks after the commencement of treatment. Interestingly, similar to the hydrogel-treated group, the mice injected with Herceptin solution (i.v.) showed 32% tumor shrinkage ($P = 0.001$) by the end of the treatment. The weekly administration of Herceptin might allow for fresh and continuous supply of the antibody, which possibly compensated for the loss of bioactivity due to proteolysis/degradation in the body system. Therapeutic efficacy of the one-time injection of Herceptin-loaded hydrogel was similar to weekly administration of Herceptin in solution (i.v.) as the polymer matrix was able to entrap the antibody and release it in a sustained manner (as seen in Section 2.4). Apoptosis and significant reduction in the number of cancer cells was observed for both treatment conditions as compared to the control without any treatment and the treatment group with s.c. injection of Herceptin solution (see green arrows, nuclei stained brown) (Figure S2B). With regards to clinical relevance, the frequency of injections can be drastically reduced via the use of hydrogel, and alongside with the convenience

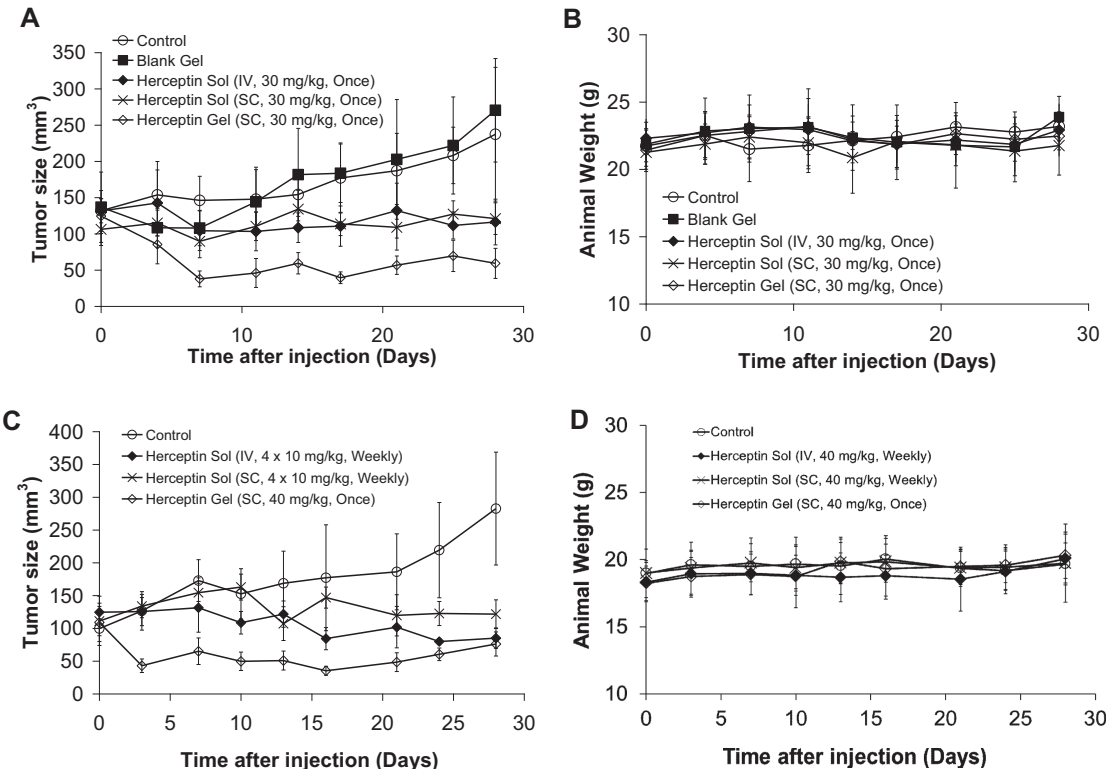

Figure 8. Changes in tumor size (A and C) and body weight (B and D) of BT474-tumor bearing mice after injection of various Herceptin formulations. Effects of one-time administration of Herceptin formulations was assessed via (A and B) while the effects of weekly administration of Herceptin solution formulations vs. one-time administration of Herceptin-loaded hydrogel was evaluated with (C and D). At the end of the treatment, two-tailed Student's t test was used to statistically evaluate the differences in the tumor volume between different formulations and also the initial and final tumor volumes of each condition. $P \leq 0.05$ indicates a statistically significant difference.

in administration, this system would be much more superior compared to other formulations and injection routes. In addition, pathological analysis of normal tissues (heart, lungs, liver and kidneys) resected from the mice used in this study revealed no toxicity as no tissue collapse or necrotic regions were seen in the treatment groups, which were similar to the control group (Figure S3). Moreover, no weight loss was observed for all mice during the course of treatments, implying good tolerance of all treatments (Figure 8D).

3. Conclusions

In this study, a biocompatible and biodegradable physically cross-linked $VitE_m$-PEG-$VitE_m$ hydrogel has been synthesized and used as an injectable local delivery material for sustained release of the antibody Herceptin. The presence of a small number of vitamin E moieties in the hydrophobic blocks is essential to allow gelation to occur at low concentrations. Rheological properties and porosity of the hydrogel can be easily adjusted by varying the chemical composition and polymer concentration. The hydrogel exhibits thixotropic property when subjected to shear stress and can recover back to a gel state almost instantly when the shear force is reduced. This reversibility of rheological behavior makes this hydrogel an excellent injectable carrier for delivery of antibodies. Histological examination reveals that the hydrogel does not induce chronic inflammatory response, and is able to degrade in vivo over time. The hydrogel matrix provides sustained release of Herceptin, and localizes the antibody within the tumor site. In vivo anti-tumor efficacy is significantly enhanced using a single subcutaneous injection of Herceptin-loaded hydrogel at a site close to the tumor as compared to Herceptin solution. Despite the anti-tumor efficacy of Herceptin-loaded hydrogel injected once at a distal site away from the tumor is comparable to that of weekly i.v. administration of Herceptin solution over 4 weeks, Herceptin treatment using the hydrogel requires much less frequent injections, providing greater convenience and improved patient compliance. These results suggest that the vitamin E-functionalized hydrogels hold great promise for subcutaneous and sustained delivery of antibodies.

4. Experimental Section

Materials: The cyclic carbonate 5-methyl-5-chlorocarbonyl-1,3-dioxan-2-one (MTC-Cl) and *N*-(3,5-trifluoromethyl)phenyl-*N'*-cyclohexylthiourea (TU) were prepared according to our previous protocol.[33] All reagents were bought from Sigma-Aldrich and used as received unless otherwise mentioned. 1,8-Diazabicyclo[5,4,0]undec-7-ene (DBU) was dried over calcium hydride and vacuum distilled twice before being transferred to a glovebox. α-Tocopherol (vitamin E) was purchased from Alfa Aesar and used as received. Herceptin (Mw: 145.5 kDa) was purchased from

Roche, Switzerland. Human dermal fibroblasts (HDF), MCF7 and BT474 human breast cancer cells were cultured in RPMI1640 medium supplemented with 10% fetal calf serum, 100 U/mL penicillin and 100 μg/mL streptomycin (HyClone, USA). 3-[4,5-Dimethylthiazol-2-yl]-2,5-diphenyl tetrazolium bromide (MTT) was obtained from Sigma, USA. MTT was dissolved in phosphate-buffered saline (PBS, pH 7.4) with a concentration of 5 mg/mL, and the solution was filtered with a 0.22 μm filter to remove blue formazan crystals prior to use.

Nuclear Magnetic Resonance (NMR) Spectroscopy: The ^{1}H-NMR spectra of monomers and polymers were recorded using a Bruker Avance 400 spectrometer, and operated at 400 MHz, with the solvent proton signal as the internal reference standard.

Molecular Weight Determination by Size Exclusion Chromatography (SEC): SEC was conducted using THF as the eluent for monitoring the polymer conversion and also for the determination of polystyrene equivalent molecular weights of the macro-transfer agents. THF-SEC was recorded on a Waters 2695D (Waters Corporation, USA) Separation Module equipped with an Optilab rEX differential refractometer (Wyatt Technology Corporation, USA) and Waters HR-4E as well as HR 1 columns (Waters Corporation, USA). The system was equilibrated at 30 °C in THF, which served as the polymer solvent and eluent with a flow rate of 1.0 mL/min. Polymer solutions were prepared at a known concentration (ca. 3 mg/mL) and an injection volume of 100 μL was used. Data collection and analysis were performed using the Astra software (Wyatt Technology Corporation, USA; version 5.3.4.14). The columns were calibrated with a series of polystyrene standards ranging from Mp = 360 Da to Mp = 778 kDa (Polymer Standard Service, USA).

Synthesis of MTC-VitE Monomers: The monomer MTC-VitE was synthesized according to a previously described protocol.[33] Briefly, MTC-OH (3.08 g, 19.3 mmol) was dissolved in anhydrous THF (50 mL) with a few drops of DMF. Oxalyl chloride (3.3 mL, 39.4 mmol) was then added dropwise and the reaction mixture stirred under a flow of nitrogen for 1 h before volatiles were removed under vacuum. The resultant off-white solid was heated to 65 °C for 2–3 min to remove any residual reagent and solvent to give the acyl chloride intermediate, MTC-Cl. The solid was redissolved in dry dichloromethane (50 mL) and chilled to 0 °C using an ice bath. A solution of α-tocopherol (8.30 g, 19.3 mmol) and dry triethylamine (3 mL, 21.6 mmol) in dry dichloromethane (50 mL) was subsequently added dropwise over 30 min. The mixture was allowed to warm up to ambient temperature and stirred for an additional 18 h. A crude solid was obtained after removal of solvent, and was subjected to purification by column chromatography using silica gel. Hexane was initially used as the eluent before gently increasing the polarity to finally end with 50% ethyl acetate. A second chromatography separation was carried out using dichloromethane/ethyl acetate (4:1) in order to obtain the desired product in high purity as a white solid (6.05 g, 53%). ^{1}H NMR (400 MHz, $CDCl_3$): δ 4.92 (d, 2H, J = 10.8 Hz, MTC-CH_2), 4.34 (d, 2H, J = 10.8 Hz, MTC-CH_2), 2.59 (d, 2H, J = 6.7 Hz, tetrahydropyrano-CH_2), 2.09 (s, 3H, Ar-CH_3), 2.00 (s, 3H, Ar-CH_3), 1.96 (s, 3H, Ar-CH_3), 1.70–1.90 (m, 2H), 1.00–1.60 (overlapping peaks, 27H), 0.80–0.90 (m, 12H, 4 × CH_3 on hydrophobic tail).

General Procedure for Polymer Synthesis: Taking Vit$E_{1.25}$-PEG(20k)-Vit$E_{1.25}$ as an example, in a 7-mL vial containing a magnetic stir bar in the glove box, MTC-VitE (58.9 mg, 100 μmol, 4.0 equiv.), HO-PEG-OH (20 kDa, 500 mg, 25 μmol, 1.0 equiv.) and TU (9.3 mg, 25 μmol, 1.0 equiv.) were dissolved in dichloromethane (4 mL). To this solution, DBU (3.7 μL, 25 μmol, 1.0 equiv.) was added to initiate polymerization. The reaction mixture was allowed to stir at room temperature and aliquots of samples were taken to monitor the monomer conversion and evolution of molecular weight by ^{1}H NMR spectroscopy and SEC. After 120 min, the reaction mixture was quenched by the addition of excess (~20 mg) of benzoic acid and was precipitated into ice-cold diethyl ether (2 × 50 mL). The resultant polymer was dried in a vial for about 1–2 days until a constant sample mass was obtained, as white powder. Selected ^{1}H NMR (400 MHz, $CDCl_3$) and GPC data of the synthesized polymers are presented as follows,

Vit$E_{1.25}$-PEG(10k)-Vit$E_{1.25}$: δ 3.40–4.00 (s, 906H, OCH_2CH_2 PEG), 1.00–2.00 (overlapping peaks, VitE), 0.75–0.95 (m, 30H, overlapping CH_3 on VitE). PDI (GPC): 1.09.

Vit$E_{2.5}$-PEG(10k)-Vit$E_{2.5}$: δ 3.40–4.00 (s, 906H, OCH_2CH_2 PEG), 1.00–2.00 (overlapping peaks, VitE), 0.75–0.95 (m, 60H, overlapping CH_3 on VitE). PDI (GPC): 1.07.

Vit$E_{1.25}$-PEG(20k)-Vit$E_{1.25}$: δ 3.40–4.00 (s, 1815H, OCH_2CH_2 PEG), 1.00–2.00 (overlapping peaks, VitE), 0.75–0.95 (m, 30H, overlapping CH_3 on VitE). PDI (GPC): 1.07.

Vit$E_{2.5}$-PEG(20k)-Vit$E_{2.5}$: δ 3.40–4.00 (s, 1815H, OCH_2CH_2 PEG), 1.00–2.00 (overlapping peaks, VitE), 0.75–0.95 (m, 60H, overlapping CH_3 on VitE). PDI (GPC): 1.12.

Vit$E_{6.5}$-PEG(20k)-Vit$E_{6.5}$: δ 3.40–4.00 (s, 1815H, OCH_2CH_2 PEG), 1.00–2.00 (overlapping peaks, VitE), 0.75–0.95 (m, 156H, overlapping CH_3 on VitE). PDI (GPC): 1.15.

Vit$E_{8.5}$-PEG(20k)-Vit$E_{8.5}$: δ 3.40–4.00 (s, 1815H, OCH_2CH_2 PEG), 1.00–2.00 (overlapping peaks, VitE), 0.75–0.95 (m, 204H, overlapping CH_3 on VitE). PDI (GPC): 1.12.

Rheological Characterization of Hydrogels: Hydrogel of known concentrations (4 to 8 wt%) was prepared by dissolving the copolymers in DI water at 25 °C. To prepare the Herceptin-loaded hydrogel, the antibody was first dissolved using sterile HPLC grade water and this solution was then added to the vitamin E-functionalized polymers for gel formation (Herceptin: 10 g/L). Rheological analysis of the gels was performed on an ARES-G2 rheometer (TA Instruments, USA) equipped with a plate-plate geometry of 8 mm diameter. Measurements were taken by equilibrating the gels at 25 °C between the plates at a gap of 1.0 mm. The data were collected under controlled strain of 0.2% and a frequency scan of 1.0 to 100 rad/s. The shear storage modulus (G′) and loss modulus (G″) of hydrogels were measured at each point. For shear-thinning studies, the viscosity of the hydrogels was monitored as a function of shear rate from 0.1 to 10 s^{-1}. From the storage modulus G′, the molar weight between the effective cross-links, Mc, was calculated using the following equation,

$$G' = \rho RT/M_c$$

where ρ is the polymer concentration [g/m^3], R is the molar gas constant, and T is the absolute temperature.[34]

Restoration of elastic modulus of hydrogel after network disruption was studied by applying high strain of 100% for 200 s and monitoring the changes in G′ and G″ at a constant frequency of 1 rad/s.

Scanning Electron Microscope (SEM) Imaging of Hydrogels: To minimize morphological perturbations, the hydrogels were cryo-fixed by transferring the sample into a chamber filled with liquid nitrogen. A day of freeze-drying process was then followed. The morphology of the gel was observed using a scanning electron microscope (SEM) (Jeol JSM-7400F, Japan).

In vitro Release of Herceptin: 0.25 mL of Herceptin-loaded hydrogels containing 10 g/L of the antibody were transferred to Transwell inserts (Corning, USA). No precipitation or leftover solution was seen after gelation, showing that all the Herceptin was loaded into the hydrogels. The inserts were then immersed in 25 mL of the release medium, i.e., PBS (pH 7.4). This was kept shaking in a water bath at 100 rpm at 37 °C. At designated time intervals, 0.1 mL of the release medium was removed and replaced with fresh medium. The released amount of Herceptin was quantified using the protein quantification BCA assay (Pierce, USA).

Cytotoxicity Study Using MTT Assay: Human dermal fibroblasts, MCF7 and BT474 cells were seeded onto 24-well plates at a density of 6 × 10^4 cells per well, and cultivated in 500 μL of growth medium. The plates were then returned to incubators for 24 h to reach ~70% confluency before treatment. When the desired cell confluency was reached, the spent growth medium was removed from each well and replaced with 500 μL of fresh medium together with 50 μL of the hydrogel in a Transwell insert and incubated for either 48 or 120 h. Each condition was tested in four replicates. When the treatment was completed, the culture medium was removed and 50 μL of MTT solution was added with 500 μL of fresh medium. The plates were then returned to the incubator and maintained in 5% CO_2, at 37 °C, for a further 3 h. The growth medium and excess MTT in each well were then removed. 600 μL of DMSO was added to each well to dissolve the internalised

purple formazan crystals. An aliquot of 100 µL was taken from each well and transferred to a new 96-well plate. The plates were then assayed at 550 nm and reference wavelength of 690 nm using a microplate reader (Tecan, USA). The absorbance readings of the formazan crystals were taken to be those at 550 nm subtracted by those at 690 nm. The results were expressed as a percentage of the absorbance of the control cells without any treatment.

In vivo Biocompatibility and Gel Degradation Studies: All animal experiments were conducted in accordance with the approved protocol from the Institutional Animal Care and Use Committee (IACUC) at the Biological Resource Centre of Singapore. Female balb/c mice, weighing 20–25 g were injected with 150 µL of blank 4 wt% $VitE_{1.25}$-(PEG20k)-$VitE_{1.25}$ hydrogel subcutaneously. At predetermined periods, mice were sacrificed and the hydrogel and its surrounding tissue were isolated. For histological examination, samples were fixed in 4% neutral buffered formalin and then stained with hematoxylin–eosin (H&E) using standard techniques. To identify the inflammatory cells populated in the subcutaneous tissue and hydrogel, immunohistochemical staining for CD45-expressing cells was carried out. The antibody used in the study was monoclonal rat anti-mouse CD45R (BD Biosciences, USA). The slides were counterstained with hematoxylin to visualize nuclei and examined using a stereomicroscope (Nikon, USA).

Biodistribution of Herceptin: To evaluate its biodistribution, Herceptin was first labeled using Alexa Fluor 790 (Invitrogen, U.S.A.). In brief, the Alexa Fluor dye with a tetrafluorophenyl (TFP) ester moiety was added to the antibody in a molar ratio of 15:1. The reaction was carried out at room temperature for 30 min. Purification of the fluorescent conjugate was carried out via ultracentrifugation. The conjugate was then analyzed using the NanoDrop ND-1000 spectrophotometer (NanoDrop Technologies, USA) and the degree of labeling was determined to be 1.45 mol Alexa Fluor dye per mole of Herceptin.

BT474 tumor-bearing female balb/c nude mice, weighing around 18–20 g, were used for this study. The mice were divided into 3 groups and administrated with 5 mg/kg Alexa Fluor790–Herceptin in different formulations: (1) hydrogel, (2) solution injected s.c. at approximately 1 cm away from the tumor site and (3) solution injected i.v. All animal experiments were conducted in accordance with the approved protocol from the Institutional Animal Care and Use Committee (IACUC) at the Biological Resource Centre of Singapore. Anesthetic animals were placed on an animal plate heated to 37 °C. The near-infrared fluorescence was imaged using the ICG filter pairs and exposure time was set to 1 s. Scans were performed at 1, 2, 3, 6, 8, 10, and 13 days post administration. The mice were sacrificed on Day 13 and organs involved in drug clearance and metabolism as well as tumor tissue were excised and imaged using IVIS (Caliper Life Science, USA).

In vivo Antitumor Efficacy Studies: All animal experiments were conducted in accordance with the approved protocol from the Institutional Animal Care and Use Committee (IACUC) at the Biological Resource Centre of Singapore. Female balb/c nude mice, weighing 18–22 g were injected with 200 µL of a cell suspension (1:1 with Matrigel) (BD Biosciences, U.S.A.) containing 5×10^6 BT474 cells subcutaneously. Three weeks after inoculation (when the tumor volume was 100–120 mm^3), the tumor-bearing mice were randomly divided into several groups (7–10 mice per group). Group 1 mice were used as nontreated control, group 2 and 3 mice were given intravenous and subcutaneous injections of Herceptin (30 mg/kg, 150 µL respectively, group 4 and group 5 mice were injected subcutaneously with blank and Herceptin-loaded hydrogel (30 mg/kg, 150 µL) respectively at ~1 cm away from the tumor site. All mice were injected only once on the first day of treatment (Day 0).

In the second set of experiment, group 1b mice were used as nontreated control, group 2b and 3b mice were given 4 doses of weekly intravenous and subcutaneous injections of Herceptin (4 × 10 mg/kg) respectively while the group 4b mice were injected once subcutaneously with Herceptin-loaded hydrogel (40 mg/kg) on the first day of treatment (Day 0) respectively. For improved clinical relevance, the s.c. injections of Herceptin solution and Herceptin-loaded hydrogel were carried out at a remote site, ~4 cm away from the tumor. The tumor size was measured by calipers in two orthogonal diameters and the volume was calculated as $L \times W^2 / 2$, where L and W are the major and minor diameters respectively. At the end of the treatment, two-tailed Student's t test was used to statistically evaluate the difference in tumor volume and $P \leq 0.05$ was considered to indicate a statistically significant difference. In addition, the toxicities of the different formulations were evaluated by monitoring the change in mouse body weight over the course of treatment.

Histological Analysis: At 28 days post injection of Herceptin formulations (Section 4.11), the mice were sacrificed and the tumors as well as normal tissues (heart, lung, liver and kidney) were individually excised and dissected. For histological examination, the samples were fixed in 4% neutral buffered formalin and then stained with hematoxylin–eosin (H&E) using standard techniques. Apoptotic cells of tumor samples were identified using Terminal Transferase dUTP Nick-End Labeling (TUNEL) assay. The slides were counterstained with hematoxylin to visualize nuclei and examined using a stereomicroscope (Nikon, USA).

Supporting Information

Supporting Information is available from the Wiley Online Library or from the author.

Acknowledgements

A. L. Z. Lee and V. W. L. Ng contributed equally to this work. This work was supported by the Institute of Bioengineering and Nanotechnology (Biomedical Research Council, Agency for Science, Technology and Research), Singapore, and IBM Almaden Research Center, USA.

Received: April 18, 2013
Revised: July 13, 2013
Published online: October 31, 2013

[1] WHO World Cancer Report 2008, http://www.iarc.fr/en/publications/pdfs-online/wcr/2008/, accessed: September, 2012.
[2] D. C. Allred, G. M. Clark, A. K. Tandon, R. Molina, D. C. Tormey, C. K. Osborne, K. W. Gilchrist, E. G. Mansour, M. Abeloff, L. Eudey, *J. Clin. Oncol.* **1992**, *10*, 599.
[3] Y. Yarden, *Oncology* **2001**, *61*, 1.
[4] R. Nahta, F. J. Esteva, *Cancer lett.* **2006**, *232*, 123.
[5] K. I. Pritchard, *J. Clin. Oncol.* **2010**, *28*, 1089.
[6] G. Ismael, R. Hegg, S. Muehlbauer, D. Heinzmann, B. Lum, S. B. Kim, T. Pienkowski, M. Lichinitser, V. Semiglazov, B. Melichar, *Lancet Oncol.* **2010**, *13*, 869.
[7] M. F. Haller, *Pharm. Techn.* **2007**, *10*, 861.
[8] D. Q. Wu, F. Qiu, T. Wang, X. J. Jiang, X. Z. Zhang, R. X. Zhuo, *ACS Appl. Mater. Interface* **2008**, *1*, 319.
[9] K. Zhang, Y. Zhang, S. Yan, L. Gong, J. Wang, X. Chen, L. Cui, J. Yin, *Acta Biomater.* **2013**, 9, 7276.
[10] T. R. Hoare, D. S. Kohane, *Polymer* **2008**, *49*, 1993.
[11] B. Jeong, Y. H. Bae, S. W. Kim, *J Biomed. Mater. Res.* **2000**, *50*, 171.
[12] K. A. Aamer, H. Sardinha, S. R. Bhatia, G. N. Tew, *Biomaterials* **2004**, *25*, 1087.
[13] I. Molina, S. Li, M. B. Martinez, M. Vert, *Biomaterials* **2001**, *22*, 363.
[14] T. Fujiwara, T. Mukose, T. Yamaoka, H. Yamane, S. Sakurai, Y. Kimura, *Macromol. Biosci.* **2001**, *1*, 204.
[15] U. Edlund, A. C. Albertsson, S. K. Singh, I. Fogelberg, B. O. Lundgren, *Biomaterials* **2000**, *21*, 945.

[16] K. J. Zhu, R. W. Hendren, K. Jensen, C. G. Pitt, *Macromolecules* **1991**, *24*, 1736.
[17] A. C. Williams, B. W. Barry, *Adv. Drug Deliv. Rev.* **2004**, *56*, 603.
[18] R. Censi, T. Vermonden, M. J. van Steenbergen, H. Deschout, K. Braeckmans, S. C. De Smedt, C. F. van Nostrum, P. Di Martino, W. E. Hennink, *J. Control. Rel.* **2009**, *140*, 230.
[19] Y. L. Chiu, S. C. Chen, C. J. Su, C. W. Hsiao, Y. M. Chen, H. L. Chen, H. W. Sung, *Biomaterials* **2009**, *30*, 4877.
[20] L. Lu, G. N. Stamatas, A. G. Mikos, *J. Biomed. Mater. Res.* **2000**, *50*, 440.
[21] X. J. Loh, S. H. Goh, J. Li, *Biomaterials* **2007**, *28*, 4113.
[22] A. McCabe, M. Dolled-Filhart, R. L. Camp, D. L. Rimm, *J. Natl. Cancer Inst.* **2005**, *97*, 1808.
[23] M. Harries, I. Smith, *Endocr. Relat. Cancer* **2002**, *9*, 75.
[24] M. A. Cobleigh, C. L. Vogel, D. Tripathy, N. J. Robert, S. Scholl, L. Fehrenbacher, J. M. Wolter, V. Paton, S. Shak, G. Lieberman, *J. Clin. Oncol.* **1999**, *17*, 2639.
[25] S. Cohen, G. Carpenter, *Proc. Natl. Acad. Sci. USA* **1975**, *72*, 1317.
[26] G. Carpenter, S. Cohen, *J.Cell Sci.* **1976**, *71*, 159.
[27] G. S. Chin, W. Liu, D. Steinbrech, M. Hsu, H. Levinson, M. T. Longaker, *Plast. Reconstr. Surg.* **2000**, *106*, 1532.
[28] V. Falanga, H. Takagi, P. I. Ceballos, J. B. Pardes, *Exp. Cell Res.* **1994**, *213*, 80.
[29] D. E. Hallahan, S. Virudachalam, *Proc. Natl. Acad. Sci. USA* **1997**, *94*, 6432.
[30] J. C. Garbern, E. Minami, P. S. Stayton, C. E. Murry, *Biomaterials* **2011**, *32*, 2407.
[31] M. Aoki, K. Okudaira, M. Haga, R. Nishigaki, M. Hayashi, *Drug Metab. Dispos.* **2010**, *38*, 1183.
[32] C. L. Litterst, E. G. Mimnaugh, R. L. Reagan, T. E. Gram, *Drug Metab. Dispos.* **1975**, *3*, 259.
[33] R. C. Pratt, F. Nederberg, R. M. Waymouth, J. L. Hedrick, *Chem. Commun.* **2008**, 114.
[34] J. W. Goodwin, R. W. Hughes, *Rheology for Chemists: An Introduction*, Royal Society of Chemistry, UK **2008**.